LAND USE AND LAND COVER SIMULATION BASED ON INTEGRATION OF ARTIFICIAL NEURAL NETWORKS WITH CELLULAR AUTOMATA-MARKOV CHAIN MODELS APPLIED TO EL-FAYOUM GOVERNORATE

Islam Atef[a], Wael Ahmed[b], Ramadan H. Abdel-Maguid[a], Moustafa Baraka[c], Walid Darwish[b,*], Ahmad M. Senousi[b]

[a] Civil Engineering Department, Faculty of Engineering, Fayoum University, Fayoum 63514, Egypt
[b] Public Works Department, Faculty of Engineering, Cairo University, Giza 12613, Egypt
[c] Civil Engineering Program, German University in Cairo, Cairo, Egypt

KEY WORDS: LULC, GIS, CA-Markov, Remote sensing, Sustainability

ABSTRACT:

The paper aims to evaluate the effectiveness of the multi-layer perceptron-Markov chain analysis (MLP-MCA) integrated method in predicting future Land Use and Land Cover (LULC) change scenarios in Fayoum due to rapid urbanization. The study employed machine learning algorithms for image classification using Google Earth Engine (GEE) for classification techniques to derive LULC maps from Landsat imagery taken in 2001, 2011, and 2021. The 2001 and 2011 LULC maps were used to predict the LULC scenario for 2021 using MLP-MCA, and the predicted result was validated against the observed 2021 LULC map using Area under the curve (AUC) that was derived from the Receiver Operating Characteristics (ROC). Subsequently, the study predicted future LULC changes for 2031 using two sub-models; sub- Agri and sub-built. The results show that a rapid growth in both built and agricultural area. The findings of this study highlight the potential of the MLP-MCA method in predicting future LULC changes due to urbanization.

1. INTRODUCTION

Land cover change is the term used to describe physical alteration of the Earth's surface, including changes in water sources, soil, and air pollution. While the land use alteration is often associated with how human behavior affects physical changes on the Earth's surface. Land use change typically has some impact on land cover change (Aburas et al., 2018). LULC Sustainability is largely concerned with changes in the environment. Human interference in the environment usually leads to changes in land use, such as deforestation, destruction of pastures, urban growth, and shrinkage of waterways (Kourosh Niya et al., 2020). These changes are leading to a shortage of natural resources, shortages in food production, and social and political impacts (Palmate et al., 2017).

Remote sensing (RS) and geographic information systems (GIS) have demonstrated great potential in studying landscape dynamics and offer provide valuable methods in the broader scope of environmental tracking (Armin et al., 2020). It is critical to simulate LULC to comprehend and recognize the potential future changes in each class of land. Planners of land use, environmentalists, and resource managers can benefit from these forecasts in order to reduce the bad impacts of planning to achieve better manage for agricultural land protection , natural resources and urban areas (Kourosh Niya et al., 2020).

In recent years, a various spatial models involved RS and GIS have been developed to predict LULC in future, such as Artificial Neural Network (ANN) model (Abbas et al., 2021), cellular automata (CA) model (Deep and Saklani, 2014), and the Conversion of Land Use and its Effects (CLUE) model (Jafarpour Ghalehteimouri et al., 2022), as a substitute, each model has drawbacks (Triantakonstantis and Mountrakis, 2012). To overcome the drawback of existing models, integration of several models had been adopted. CA-ANN is created by integrating a CA with ANN model (Abbas et al., 2021). The models provide resources for discovering spatial variation in LULC (Munthali et al., 2020). In comparison with the other models, CA-Markov Model (CA-MM) has the highest accuracy, because it can be combined many factors which effect on LULC prediction such as; biophysical, socio-economic, and remotely sensed and geospatial data (Naboureh et al., 2017). CA-MM can succefuly simulate complex patterns (Hyandye and Martz, 2017). Regmi et al. (2017) compared the CA- Markov model with the GEOMOD model for LULC future simulation and concluded that the CA-MM was more successful in future prediction than GEOMOD.Therefore, we adopted it for our prediction scenario in El-Fayoum Governorate.

The hybrid Cellular Automata-Markov Chain (CA-MC) model is a commonly used and effective method for modeling the spatiotemporal changes in LULC (Fitawok et al., 2020). The CA-MC model combines the stochastic model of CA and the technique of Markov Chain (MC) to simulate multi-directional LULC changes analysis and provide ways for projecting different future scenarios (Keshtkar and Voigt, 2015). However, Variables with explanatory power such as socioeconomic and environmental data needs to be taken into account when modeling LULC changes (Mas et al., 2014). The integration of the CA-MC model with other models, such as the Multi-Layer Perceptron Neural Network (MLP-NN), has helped to improve its prediction capability (Gharaibeh et al., 2020). MLP-NN is an effective approach that introduces a better understanding of the land change process and provides more accurate results depending on artificial intelligence. Three layers make up MLP-NN, including input, hidden layers, and output, and predicts geospatial changes with the aid of previous changes (Simwanda et

* Corresponding author

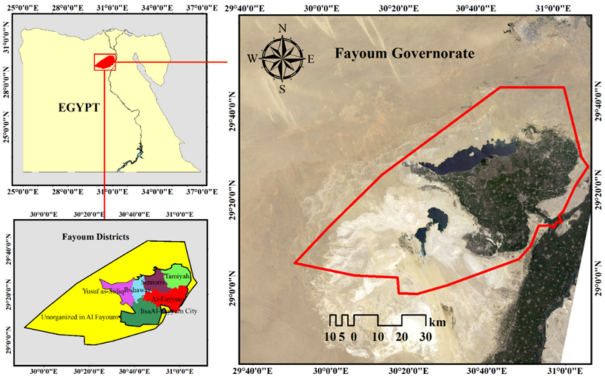

Figure 1. Fayoum Geographical location.

al., 2021). MLP-NN has the highest capability to generalize the transition potential through the backpropagation algorithm (Dey et al., 2021). The integration of MLP-NN and CA-MC (MLP-CA-MC) takes advantage of both models (Gharaibeh et al., 2020; Lamchin et al., 2022; Toma et al., 2023). MLP-NN facilitates the automatic calibration of the CA-MC model and provides a more accurate future change scenario than CA-MC alone.

In this study, the LULC trends have been refined and explained in a way that can assist and guide policymakers, land-use planners, and hydrologists for the future. Hydrology, for example, is affected differently by land use and climate change than by the separate factors, and this limits the ability to develop future water management strategies and irrigation plans. The rest of the paper is organized as follows: Section 2 describes the study area, Section 3 shows our adopted methodology to predict and simulate LULC for EL-Fayoum Governorate. Section 4 introduces the result and discussions, finally Section 5 draws the conclusion for the study.

2. STUDY AREA AND MATERIALS

El-Fayoum is in a depression in the western desert, a remarkable area. It is far from the Nile River, about 25 kilometers away, and 90 kilometers southwest of the capital of the Arab Republic of Egypt, its green land inside the desert, it draws water from the Nile via the Yusuf Sea. Figure 1 shows the location of the study area.

In this study, different LULC classes in Fayoum were mapped using digital remote sensing data from the Landsat series satellites. On GEE, the LULC maps were processed and categorized (https://code.earthengine.google.com/). Digital elevation models (DEMs) and road networks are two additional data sets used in this study. The USGS website's ASTER DEM of 30-m spatial resolution data was downloaded and used to produce slope. Google Earth image is used to extract the shape files for the roads and canals.

3. METHODOLOGY

3.1 LULC Image Classification and Assessment

Using imagery from Landsat, LULC classification maps were created. Figure 2 displays the adopted flowchart for image classification. GEE employed three different classifiers named:

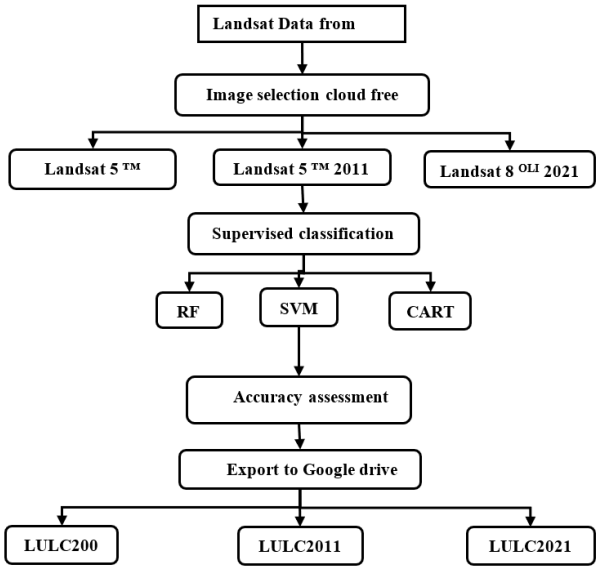

Figure 2. Adopted methodology of image classification.

support Vector Machine (SVM), Random Forest (RF), and Classification And Regression Tree (CART) as shown in Figure 2. Using the cloud mask method offered by GEE, contaminated pixels brought on by cloud cover were removed from all images (Rahman et al., 2020; Atef et al., 2023).

Four major LULC classes - agricultural land, water, bare land, and built-up - were identified and categorized in this study. By using accuracy assessment, the effectiveness and usability of classified images from 2001, 2011, and 2021 were estimated. After classification techniques were performed, an accuracy assessment was conducted to determine their accuracy. There were two types of training datasets: training and validation. Seventy percent were used for training, and thirty percent of the trained data were used for testing using a confusion matrix (Hamud et al., 2021). A built-in algorithm in GEE, called a confusion matrix, validates and rates the classification accuracy of the images using the kappa coefficient (κ) and overall accuracy (OA) (Congalton and Green, 2019).

3.2 Analysis of LULC changes

The Landsat TM/ETM+/OLI images from the years 2001, 2011, and 2021, respectively, served as the basis for the LULC changes analysis used in this study. Using the integrated software environment known as the land change modeler (LCM) for ecological sustainability, the LULC changes analysis, simulation, and LULC changes prediction were carried out (Leta et al., 2021). The LULC maps from two dates are compared to create the Markov chain matrix that serves as the foundation for the change model. Quantifying LULC changes over the periods of 2001–2011, 2011–2021, and 2001–2021 was done using cross-tabulation analysis. The LULC classes' gains and losses,

Variable name	unit	Reference
Slope	degree	Gharaibeh et al. (2020)
DEM	meter	Zhang et al. (2019)
Distance to water source	meter	Ibarra-Bonilla et al. (2021)
Distance to road	meter	Prishchepov et al. (2020)
Evidence Likelihood	dimensionless	Girma et al. (2022)

Table 1. Explanatory variables for sub-models.

as well as their contributions to the overall net change, were also examined in graphical form.

3.3 Transition potentials

For two sub-models that included specific LULC dynamics in accordance with the observed processes of change. SUB-Built is a sub model included the transition from agricultural and bare lands to built-up. SUB-Agri is a sub model included the transition from bare land to agricultural land (land reclamation). Five explanatory variables are detected form both sub models and used for transition potential map, as shown in Table 1 (Mishra and Rai, 2016).

The transition potential maps were produced using MLP. This method can generate transition potentials across non-linear function simulation algorithms (Saha et al., 2022). The MLP parameters were employed in this study: 10,000 iterations, 50% training and 50% testing samples, 0.001 learning rate, 0.01 momentum factor, and 10 hidden layers. The effectiveness of the transition potentials in both sub-models was evaluated using the accuracy rate and skill measure outcomes of the training methods in the MLP.

3.4 Future Simulation and assessment

The MC procedure from the LCM was used to model potential future scenarios, as shown in Figure 3. The MC process was utilized to simulate LULC in 2031, which is 10 years from 2021 compared to the identical time lapse that existed between 2001 and 2021. The probability matrix of transitions from 2001 to 2021 and the transition potentials of each created sub-model: SUB-Built and SUB-Agri were the main focus of the simulation process. Based on the (ROC) approach, the future scenarios were validated (Rahnama, 2021). Area under the curve (AUC), derived from the ROC, is also used to assess our scenarios' validity. It was considered satisfactory if the AUC exceeded 0.5 (Ibarra-Bonilla et al., 2021).

4. RESULTS AND DISCUSSION

4.1 Image classification

For choosing the best classifier we used imagery in 2021, a total of 425 training samples were used, training samples was greater than 70% of sample. The testing sample was smaller or equal

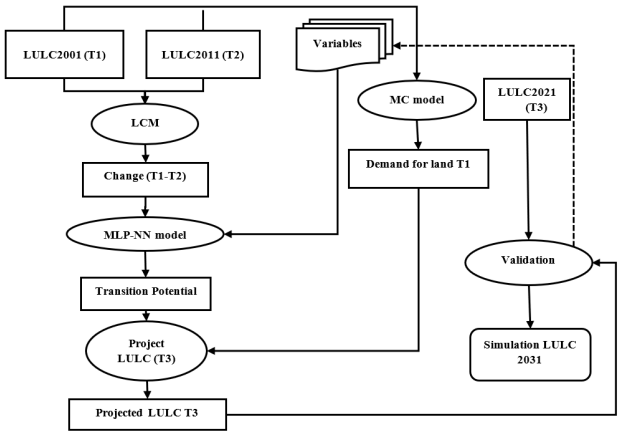

Figure 3. Adopted Flowchart for future prediction.

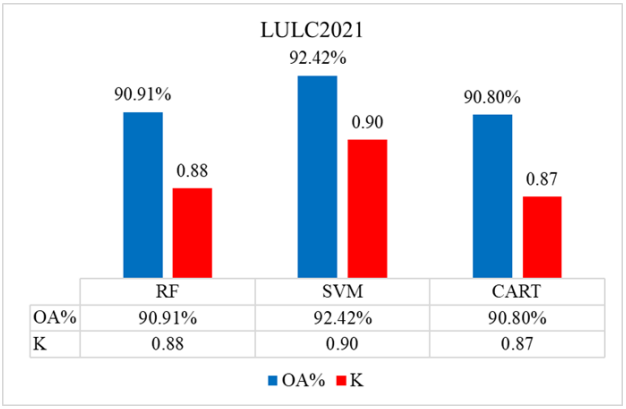

Figure 4. Comparison between image classification algorithms: random forest (RF), support vector Machine (SVM), and classification and regression tree (CART).

30% of total samples. Every classification class should typically have at least 50 training samples (Freund and Schapire, 1997). We used overall (OA) and κ for testing accuracy (Khwarahm et al., 2021). SVM -as shown in Figure 4 - got the high OA and κ results, so it was applied to 2001, 2011, and 2021 for image classification.

4.2 Analysis of Changes in LULC

Over the past decade, there have been massive changes to LULC classes. Table 2 shows the amounts of changes in LULC from 2001 to 2021. It could be found that the extreme changes occurred to Built-Up area which represented 3.74% of governorate area. It was changed 5.38% in the first decade from 2001 to 2011 while sudden increase occurred in the period from 2011 to 2021 and the total area increased by 43.08%. The spatiotemporal analysis from image classification shown in Figure 5 demonstrates that this expansion due to reduction in the agriculture land. While agriculture class increased 2.28% in 2011 and 1.88% in 2021. The expansion of built-up and agriculture due to the reduction in bare land that reduced by 0.79% in 2011 and 2.93 % in 2021. Water and bare land experienced a decline during this time. Built-up area increased dynamically during the study period due to population growth and the high demand for land and urban resources. Additionally, it is evident that water bodies in the study area have drastically decreased between

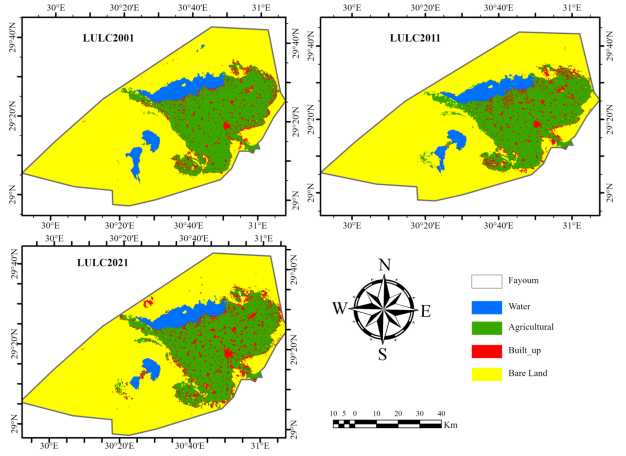

Figure 5. LULC maps for the years 2001, 2011, 2021.

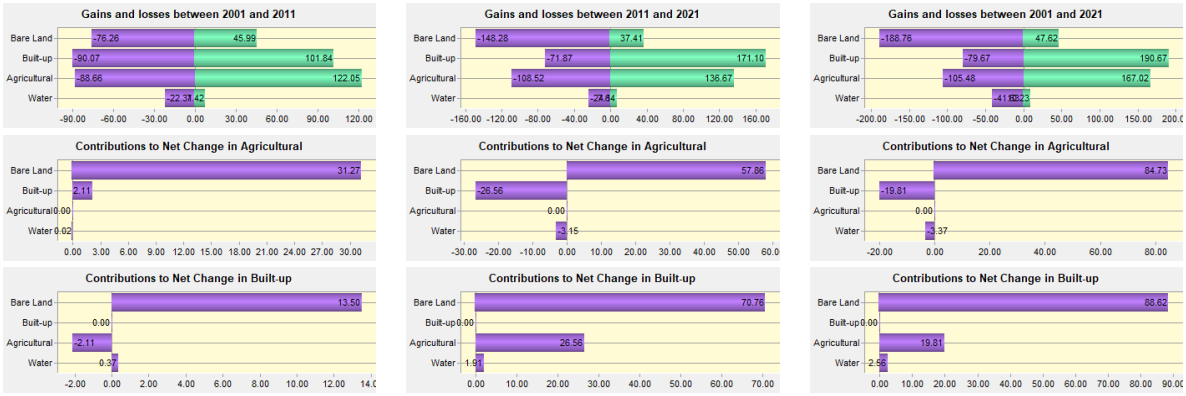

(2001-2011) (2011-2021) (2001-2021)

Figure 6. Gain and loss in km^2 and net change contributions for each period.

Classes \ Change Period	2001(Area (Km^2))	2001-2011 (%)	2011-2021 (%)	2001-2021 (%)
Water	350.28 (5.99%)	-4.25	-4.93	-8.96
Agricultural	1463.38 (25%)	2.28	1.88	4.21
Built-up	218.60 (3.74%)	5.38	43.08	50.78
Bare Land	3819.63 (65.27%)	-0.79	-2.93	-3.70

Table 2. Change Rates of LULC from 2001 to 2021.

2001 and 2021 by 8.96%.

4.3 LULC changes analysis using LCM

By using LCM's change analysis tool, the LULC maps of 2001, 2011, and 2021 were also analyzed for periods 1, 2, and 3. Different classes' losses and gains were evaluated when evaluating LULC changes. Both gains and losses are shown in Figure 6. Figure 7 shows the change maps from 2001-2021. During period 1, the bare land has lost 76.26 km^2 and increased by 45.99 km^2, resulting in a net loss of 30.27 km^2. The net loss of water category is 14.89 km^2, with 22.31 km^2 lost and 7.42 km^2 gained. There has been a loss of 90.07 km^2 and a gain of 101.84 km^2 in the built-up area with a net gain of 11.77 km^2. With a net gain of 33.39 km^2, agricultural land has gained 122.05 km^2 while losing 88.66 km^2. While in period 2, the bare land has lost 148.28 km^2 and increased by 37.41 km^2, resulting in a net loss of 110.87km^2. The net loss of water category is 16.52 km^2, with 24.16 km^2 lost and 7.64 km^2 gained. There has been a loss of 71.87 km^2 and a gain of 171.10 km^2 in the built-up area with a net gain of 99.23 km^2. With a net gain of 28.15 km^2, agricultural land has gained 136.67 km^2 while losing 108.52 km^2. For period 3, the bare land has lost 188.76 km^2 and increased by 47.62 km^2, resulting in a net loss of 141.14 km^2. The net loss of water category is 111 km^2, with 41.63km^2 lost and 10.23 km^2 gained. There has been a loss of 71.87 km^2 and a gain of 171.10 km^2 in the built-up area with a net gain of 99.23 km^2. With a net gain of 61.54 km^2, agricultural land has gained 167.02 km^2 while losing 105.48 km^2. Agricultural land has gained 167.02 km^2 while losing 105.48 km^2 with net gain of 61.54 km^2.

4.4 MLP-NN skill measure

MLP-NN is a machine learning techniques that has the ability to effectively model sophisticated patterns and conduct, as previously demonstrated by (Gharaibeh et al., 2020). In this study, two sub-models were developed using MLP-NN, each consisting of one input layer, one hidden layer, and one output layer Table 6 . The input layer contained seven driver variables, while the hidden layer contained ten nodes for both SUB-Built and SUB-Agri. The output layer for SUB-Built and SUB-Agri contained four and two nodes, respectively. The nodes in each layer were interconnected through varying weights. To assess the impact and order of influence of each driver variable, 1,000 iterations were performed, and three sensitivity analyzation techniques were utilized. As detailed in the subsequent subsections. The goal of network training was to determine the optimal weights for the connections between the input and hidden layers, as well as between the hidden and output layers, to enable accurate classification of unknown pixels.

For the generation of transition potential maps (TPM), variables previously tested were applied for both sub-models. Thus, for SUB-built and SUB-Agri, all the variables were applied. With this, the accuracy rate increased to 71.00% and 86.78%, for SUB-built and SUB-Agri, respectively as shown in Figure 8. In this study, the results indicated an acceptable accuracy, despite the lowest value detected for SUB-built. Islam and Ahmed

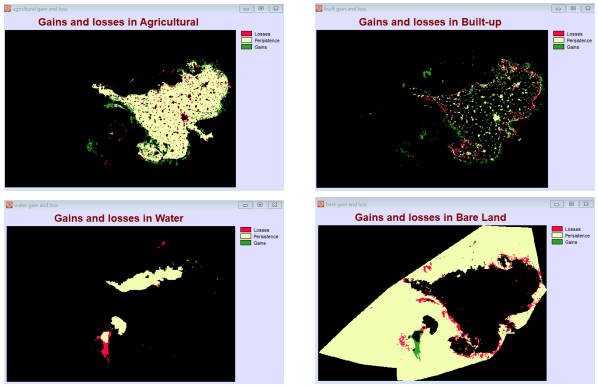

Figure 7. Alteration of Gains and losses in LULC during 2001–2021.

Parameter	SUB-Built	SUB-Agri
Input layer neurons	5	5
Hidden layer neurons	10	10
Output layer neurons	4	2
Requested samples per class	10000	10000
Final learning rate	0.001	0.001
Momentum factor	0.01	0.01
Sigmoid constant	1	1
Acceptable RMS	0.01	0.01
Iterations	1000	1000
Training RMS	0.3037	0.3094
Testing RMS	0.3062	0.3100
Accuracy rate	71.00%	86.78%

Table 3. Explanatory variables for sub-models.

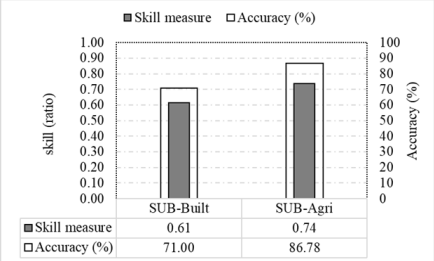

Figure 8. Each sub-model accuracy rate and skill measure.

(2012) suggest that values of accuracy for neural network processes should reach up to 70%; however, this result will depend to the influence of used variables. The accuracies for the sub-models of this study were considered effective. TMP revealed that bare land had the highest probability of persistence, and that the LULC class with the lowest probability of persistence was built up Table 4.

2001-2011	Water	Agricultural	Built-up	Bare land
Water	0.94	0.01	0.00	0.05
Agricultural	0.00	0.94	0.05	0.01
Built-up	0.00	0.34	0.59	0.07
Bare Land	0.00	0.01	0.01	0.98

Table 4. TPM of LULC changes from 2001 to 2011.

4.5 Projected of LULC for 2031

After forecasting the LULC 2021 (i.e., 10 years from 2011), based on TPM for the lapse of 2001 (time 1) and 2011 (time 2), as well as the transition potentials of each generated sub-model (SUB-Built and SUB-Agri), The ROC result showed that the sub-model AUC was greater in every scene than the random baseline value, indicating successful projections (Figure 9). SUB-Built performance was the best even though it was created with the fewest explanatory variables (AUC = 0.686); however, SUB-Agri performance was significantly worse than those of SUB-Built even though they included more explanatory variables. Then we used 2011 as time 1 and 2021 as time 2 to forecast 2031 based on TPM from 2011–2021 (as shown in Table 5).

When we compared the two sub-models in 2031, using the

2011-2021	Water	Agricultural	Built-up	Bare land
Water	0.93	0.01	0.01	0.06
Agricultural	0.00	0.93	0.06	0.01
Built-up	0.00	0.28	0.69	0.03
Bare Land	0.00	0.02	0.02	0.96

Table 5. TPM of LULC changes from 2011 to 2021.

Sub-model 2031	SUB-Agri		SUB-Built	
Category	Km^2	(%) change 2021-2031	Km^2	(%) change 2021-2031
Water	318.88	0.00%	318.88	0.28%
Agricultural	1592.61	4.44%	1432.21	-6.47%
Built-up	329.60	0.00%	497.36	33.73%
Bare Land	3610.81	-1.84%	3603.45	-2.08%

Table 6. LULC Projected for 2031 for Sub-Agriculture and Sub-Building.

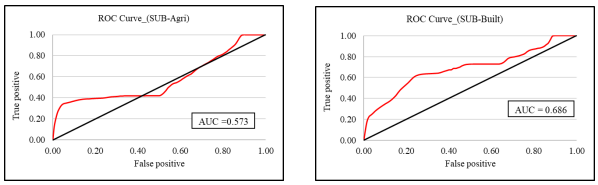

Figure 9. ROC curve and AUC for two sub-models.

changes from 2021, the predicted scenarios revealed the findings in LULC (shown in Table 6). SUB-Agri predicted that agriculture's surface would increase by 4.44%. The class of Bare Land showed the biggest loss (1.84%). SUB-built modeling revealed that agriculture will reduce its surface by 6.47%. In contrast, the built-up will rise (33.73%).

5. CONCLUSIONS

The study determined how LULC patterns altered in the Fayoum, Egypt, study area between 2001 and 2021. Agricultural encroachment and population growth are two of the biggest factors affecting land use changes. Recognizing past harmful trends is crucial to improving sustainable urban management and planning. Crop yields and temperatures can be negatively affected by changing LULC patterns. A variety of classifiers on GEE were applied to the LULC classification problem, including support vector machines (SVM), random forests (RF), and classification and regression trees (Cart). SVMs were capable of capturing land cover alterations and trends accurately. In terms of the change rate in agricultural lands from 2001 to 2021, we observe a total change rate of 4.21%. Agricultural land conversion and urban settlement are the primary drivers of land-use change in Fayoum between 2011 and 2021. However, land reclamation in the desert made up for this shortfall. There was a change rate of 50.78% in built-up from 2001 to 2021. Bare land classes showed minimal change rates. Two sub-models (SUB-Agri and SUB-Built) were simulated by CA-ANN in 2031. The SUB-Agri model predicted an increase in agricultural land and a decline in bare land. According to the SUB-Built model, built-up land increased and agricultural land declined. It is especially concerning that urbanization and fragmentation of agriculture may result in sharp changes in LULC that could place the environment, natural resources, and food security at risk. Rapid built-up will significantly affect agricultural production. The results of the spatiotemporal and potential LULC simulation may therefore give decision-makers a greater awareness of how socioeconomic factors affect changes in LULC intensity as well as a more solid foundation for environmental preservation and a more sustainable future. Future research should examine the impact of climatic changes caused by the rapid rate of built-up expansion and the scale of economic gains indicated by built-up expansion and land use permitting.

References

Abbas, Z., Yang, G., Zhong, Y., Zhao, Y., 2021. Spatiotemporal Change Analysis and Future Scenario of LULC Using the CA-ANN Approach: A Case Study of the Greater Bay Area, China.

Aburas, M. M., Ho, Y. M., Ramli, M. F., Ash'aari, Z. H., 2018. Monitoring and assessment of urban growth patterns using spatio-temporal built-up area analysis. *Environmental Monitoring and Assessment*, 190(3), 156.

Armin, M., Majidian, M., Kheybari, V. G., 2020. Land Use/Land Cover Change Detection and Prediction in the Yasouj City Suburbs in Kohgiluyeh Va Boyerahmad Province in Iran. *Arid Ecosystems*, 10(3), 203–210.

Atef, I., Ahmed, W., Abdel-Maguid, R. H., 2023. Modelling of land use land cover changes using machine learning and GIS techniques: a case study in El-Fayoum Governorate, Egypt. *Environmental Monitoring and Assessment*, 195(6), 637.

Congalton, R. G., Green, K., 2019. *Assessing the accuracy of remotely sensed data: principles and practices*. CRC press.

Deep, S., Saklani, A., 2014. Urban sprawl modeling using cellular automata. *The Egyptian Journal of Remote Sensing and Space Science*, 17(2), 179–187.

Dey, N. N., Al Rakib, A., Kafy, A. A., Raikwar, V., 2021. Geospatial modelling of changes in land use/land cover dynamics using Multi-layer Perceptron Markov chain model in Rajshahi City, Bangladesh. *Environmental Challenges*, 4, 100148.

Fitawok, M. B., Derudder, B., Minale, A. S., Van Passel, S., Adgo, E., Nyssen, J., 2020. Modeling the Impact of Urbanization on Land-Use Change in Bahir Dar City, Ethiopia: An Integrated Cellular Automata–Markov Chain Approach.

Freund, Y., Schapire, R. E., 1997. A decision-theoretic generalization of on-line learning and an application to boosting. *Journal of computer and system sciences*, 55(1), 119–139.

Gharaibeh, A., Shaamala, A., Obeidat, R., Al-Kofahi, S., 2020. Improving land-use change modeling by integrating ANN with Cellular Automata-Markov Chain model. *Heliyon*, 6(9).

Girma, R., Fürst, C., Moges, A., 2022. Land use land cover change modeling by integrating artificial neural network with cellular Automata-Markov chain model in Gidabo river basin, main Ethiopian rift. *Environmental Challenges*, 6, 100419.

Hamud, A. M., Shafri, H. Z. M., Shaharum, N. S. N., 2021. Monitoring Urban Expansion And Land Use/Land Cover Changes In Banadir, Somalia Using Google Earth Engine (GEE). *IOP Conference Series: Earth and Environmental Science*, 767(1), 12041.

Hyandye, C., Martz, L. W., 2017. A Markovian and cellular automata land-use change predictive model of the Usangu Catchment. *International Journal of Remote Sensing*, 38(1), 64–81.

Ibarra-Bonilla, J. S., Villarreal-Guerrero, F., Prieto-Amparán, J. A., Santellano-Estrada, E., Pinedo-Alvarez, A., 2021. Characterizing the impact of Land-Use/Land-Cover changes on a Temperate Forest using the Markov model. *The Egyptian Journal of Remote Sensing and Space Science*, 24(3, Part 2), 1013–1022.

Islam, M. S., Ahmed, R., 2012. Land Use Change Prediction In Dhaka City Using Gis Aided Markov Chain Modeling. *Journal of Life and Earth Science*, 6(0 SE - Articles), 81–89.

Jafarpour Ghalehteimouri, K., Shamsoddini, A., Mousavi, M. N., Binti Che Ros, F., Khedmatzadeh, A., 2022. Predicting spatial and decadal of land use and land cover change using integrated cellular automata Markov chain model based scenarios (2019–2049) Zarriné-Rūd River Basin in Iran. *Environmental Challenges*, 6, 100399.

Keshtkar, H., Voigt, W., 2015. A spatiotemporal analysis of landscape change using an integrated Markov chain and cellular automata models. *Modeling Earth Systems and Environment*, 2(1), 10.

Khwarahm, N. R., Qader, S., Ararat, K., Fadhil Al-Quraishi, A. M., 2021. Predicting and mapping land cover/land use changes in Erbil /Iraq using CA-Markov synergy model. *Earth Science Informatics*, 14(1), 393–406.

Kourosh Niya, A., Huang, J., Kazemzadeh-Zow, A., Karimi, H., Keshtkar, H., Naimi, B., 2020. Comparison of three hybrid models to simulate land use changes: a case study in Qeshm Island, Iran. *Environmental Monitoring and Assessment*, 192(5), 302.

Lamchin, M., Lee, W.-K., Wang, S. W., 2022. Multi-Temporal Analysis of Past and Future Land-Cover Changes of the Third Pole. *Land*, 11(12), 2227.

Leta, M. K., Demissie, T. A., Tränckner, J., 2021. Modeling and Prediction of Land Use Land Cover Change Dynamics Based on Land Change Modeler (LCM) in Nashe Watershed, Upper Blue Nile Basin, Ethiopia.

Mas, J.-F., Kolb, M., Paegelow, M., Camacho Olmedo, M. T., Houet, T., 2014. Inductive pattern-based land use/cover change models: A comparison of four software packages. *Environmental Modelling Software*, 51, 94–111.

Mishra, V. N., Rai, P. K., 2016. A remote sensing aided multilayer perceptron-Markov chain analysis for land use and land cover change prediction in Patna district (Bihar), India. *Arabian Journal of Geosciences*, 9(4), 249.

Munthali, M. G., Mustak, S., Adeola, A., Botai, J., Singh, S. K., Davis, N., 2020. Modelling land use and land cover dynamics of Dedza district of Malawi using hybrid Cellular Automata and Markov model. *Remote Sensing Applications: Society and Environment*, 17, 100276.

Naboureh, A., Rezaei Moghaddam, M. H., Feizizadeh, B., Blaschke, T., 2017. An integrated object-based image analysis and CA-Markov model approach for modeling land use/land cover trends in the Sarab plain. *Arabian Journal of Geosciences*, 10(12), 259.

Palmate, S. S., Pandey, A., Mishra, S. K., 2017. Modelling spatiotemporal land dynamics for a trans-boundary river basin using integrated Cellular Automata and Markov Chain approach. *Applied Geography*, 82, 11–23.

Prishchepov, A. V., Schierhorn, F., Dronin, N., Ponkina, E. V., Müller, D., 2020. 800 Years of Agricultural Land-use Change in Asian (Eastern) Russia BT - KULUNDA: Climate Smart Agriculture: South Siberian Agro-steppe as Pioneering Region for Sustainable Land Use. Springer International Publishing, Cham, 67–87.

Rahman, A., Abdullah, H. M., Tanzir, M. T., Hossain, M. J., Khan, B. M., Miah, M. G., Islam, I., 2020. Performance of different machine learning algorithms on satellite image classification in rural and urban setup. *Remote Sensing Applications: Society and Environment*, 20, 100410.

Rahnama, M. R., 2021. Simulation of land use land cover change in Melbourne metropolitan area from 2014 to 2030: using multilayer perceptron neural networks and Markov chain model. *Australian Planner*, 57(1), 36–49.

Regmi, R. R., Saha, S. K., Subedi, D. S., 2017. Geospatial Analysis of Land Use Land Cover Change Modeling in Phewa Lake Watershed of Nepal by Using GEOMOD Model. *Himalayan Physics*, 6(0 SE - Articles), 65–72.

Saha, P., Mitra, R., Chakraborty, K., Roy, M., 2022. Application of multi layer perceptron neural network Markov Chain model for LULC change detection in the Sub-Himalayan North Bengal. *Remote Sensing Applications: Society and Environment*, 26, 100730.

Simwanda, M., Murayama, Y., Phiri, D., Nyirenda, V. R., Ranagalage, M., 2021. Simulating Scenarios of Future Intra-Urban Land-Use Expansion Based on the Neural Network–Markov Model: A Case Study of Lusaka, Zambia.

Toma, M. B., Belete, M. D., Ulsido, M. D., 2023. Historical and future dynamics of land use land cover and its drivers in Ajora-Woybo watershed, Omo-Gibe basin, Ethiopia. *Natural Resource Modeling*, 36(1), e12353.

Triantakonstantis, D., Mountrakis, G., 2012. Urban growth prediction: a review of computational models and human perceptions.

Zhang, D., Liu, X., Wu, X., Yao, Y., Wu, X., Chen, Y., 2019. Multiple intra-urban land use simulations and driving factors analysis: a case study in Huicheng, China. *GIScience Remote Sensing*, 56(2), 282–308.